ISSN 1063-7834, Physics of the Solid State, 2018, Vol. 60, No. 7, pp. 1338–1343. © Pleiades Publishing, Ltd., 2018.
Original Russian Text © E.A. Mikhaleva, I.N. Flerov, A.V. Kartashev, M.V. Gorev, M.S. Molokeev, L.N. Korotkov, E. Rysiakiewicz-Pasek, 2018, published in Fizika Tverdogo Tela, 2018, Vol. 60, No. 7, pp. 1328–1333.

FERROELECTRICITY

Specific Heat and Thermal Expansion of Triglycine Sulfate–Porous Glass Nanocomposites

E. A. Mikhaleva[a, *], I. N. Flerov[a, b], A. V. Kartashev[a, c], M. V. Gorev[a, b], M. S. Molokeev[a, b, d], L. N. Korotkov[e], and E. Rysiakiewicz-Pasek[f]

[a] *Kirensky Institute of Physics, Krasnoyarsk Scientific Center, Siberian Branch, Russian Academy of Sciences, Krasnoyarsk, 660036 Russia*

[b] *Siberian Federal University, Institute of Engineering Physics and Radio Electronics, Krasnoyarsk, 660041 Russia*

[c] *Krasnoyarsk State Pedagogical University, Krasnoyarsk, 660060 Russia*

[d] *Far Eastern State Transport University, Khabarovsk, 680000 Russia*

[e] *Voronezh State Technical University, Voronezh, 394000 Russia*

[f] *Division of Experimental Physics, Faculty of Fundamental Problems and Technology, Wroclaw University of Science and Technology, 50-370 Wroclaw, Poland*

**e-mail: katerina@iph.krasn.ru*

Received February 1, 2018

Abstract—The effect of restricted geometry on specific heat capacity and thermal expansion of the triglycine sulfate (TGS)–borosilicate glass composites have been studied first. A decrease in the entropy and temperature of the $P2_1 \leftrightarrow P2_1/m$ phase transition in the TGS component with decreasing the glass matrix pore diameter at the invariable specific heat and thermal expansion coefficient has been observed. The estimates are indicative of the minor effect of internal pressure on the TGS pressure coefficient dT_C/dp in the composites.

DOI: 10.1134/S1063783418070181

1. INTRODUCTION

The increased interest in composite materials is due to the following factors. First, it is mostly evoked by the possibility of studying materials of different physical natures (ferroelectrics, ferromagnets, and ferroelastics) under special conditions, which can only be ensured by forming a composite. Second, many substances exhibit useful characteristics that give ground to designing a wide range of functional elements for different fields of engineering, the efficiency of which in a composite material can be significantly higher. The latter circumstance is confirmed by numerous experimental studies, which revealed the strong influence of size factors on the properties of a composite active element. In other words, the properties of a substance can be significantly changed during the transition from bulk single crystals to micrometer/nanometer crystals, films, ceramics, and composites [1].

Specific features of composite materials are the absence of chemical interaction between elements and the presence of a sharp interface between crystalline phases.

There are several ways of forming ferroic and multiferroic composites [2]. The most widespread of them is mechanical mixing of grinded components with the subsequent preparation of ceramic samples. This process is time-consuming, since it suggests controlling the particle size and ceramic sample density, which determine the degree of elastic interaction between components [3, 4]. Another widely used method includes fabrication of single- and multilayer hybrid thin films based, e.g., on the piezoelectric and magnetic oxides [1]. This method allows the component particle size and layer thickness to be specified in advance. However, in this case, the interaction of components is superficial. Preparation of components by embedding substances into a porous matrix (passive element) ensures the more extensional interaction between them.

As a matrix frame, high-strength rigid materials, e.g., borosilicate glasses, SiO_2, $A1_2O_3$, etc., are often used, in which strictly directed or random pores with a controlled diameter from several angstroms to micrometers can be formed [1]. Numerous literature data show that among ferroic materials ferroelectrics are the most convenient for embedding, which can be used to easily prepare a saturated aqueous solution. The matrix is impregnated with the aqueous solution and, upon subsequent drying, a ferroelectric crystal forms in the pores, thereby leading to the fairly tight binding between pore walls and crystallites.

Table 1. Some parameters of porous PG matrices and TGS + PG nanocomposites

Pore size d_{pore}, nm	Glass porosity, %	Filling factor, %	Crystallite size, nm	Unit cell volume TGS, nm
46	55	50	74(4)	0.64090(34)
160	46	61	133(4)	0.64092(10)
320	50	58	133(6)	0.64141(10)
320	50	48	168(6)	0.641019(56)
Bulk TGS				0.642424(58)

Although the range of ferroelectrics embedded into pores of different matrices is fairly wide ($NaNO_2$ [5], $Na_{1-x}K_xNO_2$ [6], KDP [7, 8], ADP [8], NH_4HSO_4 [9], TGS [10], etc.), the studies were often aimed at establishing the character and degree of influence of the limited geometry (matrix type and pore size) on the dielectric properties of composites [5, 6, 8–17]. At the same time, the studies of thermal properties of the ferroelectric–matrix composites, which brought useful information on some important characteristics of the phase transitions, including the entropy, thermal expansion, and sensitivity to the high external pressures, have been carried out episodically and only by pilot methods [5, 7, 8]. Only recently we carried out thorough investigations of the specific heat, elastic deformation, thermal expansion coefficients, and temperature–pressure phase diagram for a number of NH_4HSO_4–borosilicate glass nanocomposites with pore sizes of 46–320 nm [18]. The results obtained allowed us to establish the degree and character of the pore size effect on the temperature, type, entropy, deformation, permittivity, and pressure coefficients at the sequential phase transitions $P\text{-}1 \leftrightarrow Pc \leftrightarrow P2_1$. In addition, we analyzed and compared the effects of internal (caused by the elastic interaction of components) and external hydrostatic pressures. The phase transitions in NH_4HSO_4 represent brightly pronounced first- ($P\text{-}1 \leftrightarrow Pc$) and second-order ($Pc \leftrightarrow P2_1$) transformations. Of undoubted interest is studying the effect of limited geometry on ferroelectrics undergoing a phase transition near the tricritical point, when the heat properties exhibit considerable anomalies, while the latent of heat transition is absent. Therefore, the chosen ferroelectric component is triglycine sulfate (TGS), in which such a ferroelectric phase transition ($P2_1 \leftrightarrow P2_1/m$) occurs at $T_C = 321.4$ K and is accompanied by the significant entropy variation $\Delta S = 6.78$ J/mol K $= 0.815R$ [19]. When studying various properties of TGS embedded in different porous matrices, except for the thermal properties, the following specific features were established [10–13, 15, 17]: (i) the embedded TGS retains the ferroelectric state below T_C, (ii) there is the TGS texture in Al_2O_3 matrix pores, (iii) a decrease in the pore size is accompanied by an increase in the TGS unit cell volume as compared with a value for the bulk single crystal, (iv) a significantly spread phase transition is observed, and (v) the transition temperature changes nonmonotonically with decreasing pore size: T_C first increases and, starting from 70 nm, decreases and becomes lower than in bulk TGS [15].

In this work, we investigated specific heat and thermal expansion of some TGS–borosilicate glass composites and a TGS ceramic sample prepared from a material embedded in the matrix. The effect of limited geometry and size factors on the thermal characteristics of the phase transition in TGS was examined.

2. EXPERIMENTAL

Hereinafter, the borosilicate porous glasses are referred to as PG and the TGS–glass composites, as TGS + PG.

Before fabrication of the composites, we grew a bulk TGS single crystal from the aqueous solution under the maximally equilibrium temperature conditions. A quasi-ceramic sample was prepared from the crystal by tableting a fine powder without subsequent annealing and used in the analogous temperature investigations as those conducted on the composites.

Characterization of TGS was performed at room temperature using a Bruker D8 ADVANCE X-ray powder diffractometer (Cu-K_α radiation). The X-ray diffraction pattern (Fig. 1a) contains no reflections that would indicate the presence of foreign phases and impurities in the initial crystal.

The borosilicate glasses with an average pore diameter of 46, 160, and 320 nm were chosen as matrices. The glass samples were rectangular plates about 10.0 × 10.0 × 0.5 mm in size. The samples were certified using a procedure described in [20]. The porosity of all glasses was about 50% (Table 1).

TGS was embedded in the matrix by immersing the dried glasses in a saturated TGS aqueous solution at a temperature of 70°C and exposure for ~(10–20) min. Further cooling to room temperature was performed at the low rate (~0.1 K/min). The filled glasses were thoroughly dried at 100°C. After each drying, the glass surface was cleaned by mechanical polishing from the remaining crystals formed during crystallization and drying. The cycle was repeated 5–8 times. The degree of filling was estimated as a ratio between the embedded TGS and pore volumes (Table 1). The masses of

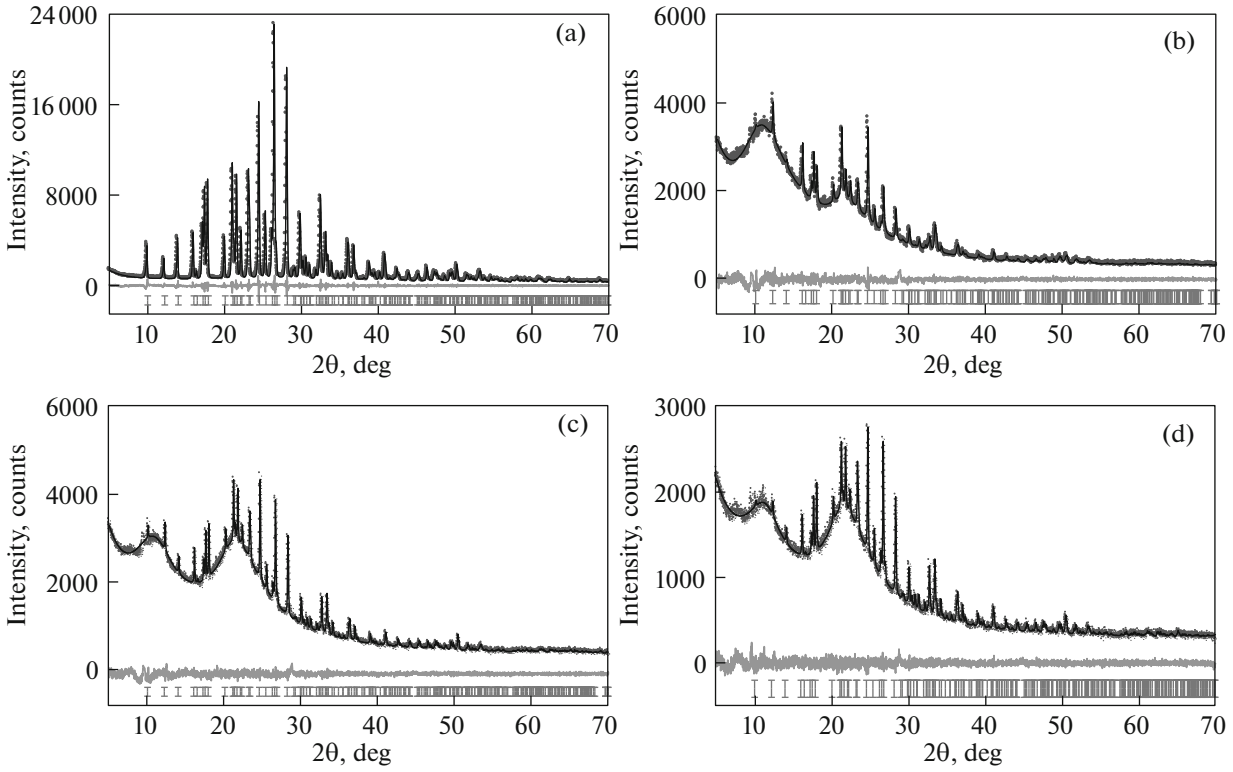

Fig. 1. XRD patterns: (a) TGS, (b) TGS + PG46, (c) TGS + PG160, and (d) TGS + PG320.

the investigated composites were close to each other and changed within 79–86 mg.

The results of Rietveld refinement of the structural model of the TGS + PG46, TGS + PG160, and TGS + PG320 composites are shown in Figs. 1b, 1c, and 1d. It can be seen that there are TGS crystals in the matrix pores without foreign phases and inclusions. The presence of two halos in the X-ray patterns is related to the amorphous state of the glasses.

Analysis of the X-ray data using the TOPAS 4.2 program [21] allowed us to determine the crystallite size d_{cryst} in the glass matrix pores (Table 1). It was found that d_{cryst} is larger than the pore dimeter d_{pore} only in the TGS + PG46 composite, as was observed in other studies, where this fact was attributed to the formation of dendritic clusters [14, 15]. One may assume that, in the case of TGS + PG160 and TGS + PG320, the ferroelectric does not completely fill the pore volume and has a reliable contact with the pore walls. This is indicated by the trend to a decrease in the unit cell volume V_{cell} of embedded TGS in comparison with the free bulk crystal.

Note a minor difference between the parameters of the two TGS + PG320 samples prepared in independent experiments, which is indicative of the reproducibility of filling the matrix with the ferroelectric component (Table 1).

Specific heat $C_p(T)$ of the composites and ceramic TGS in a wide temperature range and near the phase transition was investigated on an automated adiabatic calorimeter used by us in studying the NH_4HSO_4 glass composites [18] (see the description in [22]). The experiments were carried out in high vacuum (the residual pressure is 10^{-6} Torr) upon discrete (with a step of 1–3 K) and continuous ($dT/dt \approx 0.15$–0.30°C/min) heating. The specific heat determination error was no higher than 0.5–1.0%.

The temperature dependences of specific heat of a heating agent, contact lubricant, and PG were determined in separate experiments. The anomalous behavior was not observed. The difference between the specific heat values of the glasses studied was no more than 2%.

Thermal expansion was investigated on an NETZSCH DIL-402C dilatometer in the temperature range of 100–370 K in the dynamic mode at a temperature variation rate of 3°C/min. All the measurements were performed in the helium atmosphere. Fused quartz references were used in calibrating and accounting for the expansion of the measuring system.

The preliminarily measurements on glasses showed a very small (no higher than 5×10^{-6} K^{-1}) thermal expansion coefficient in the investigated temperature range and the absence of anomalous behavior. Owing to the large difference between the PG and TGS ther-

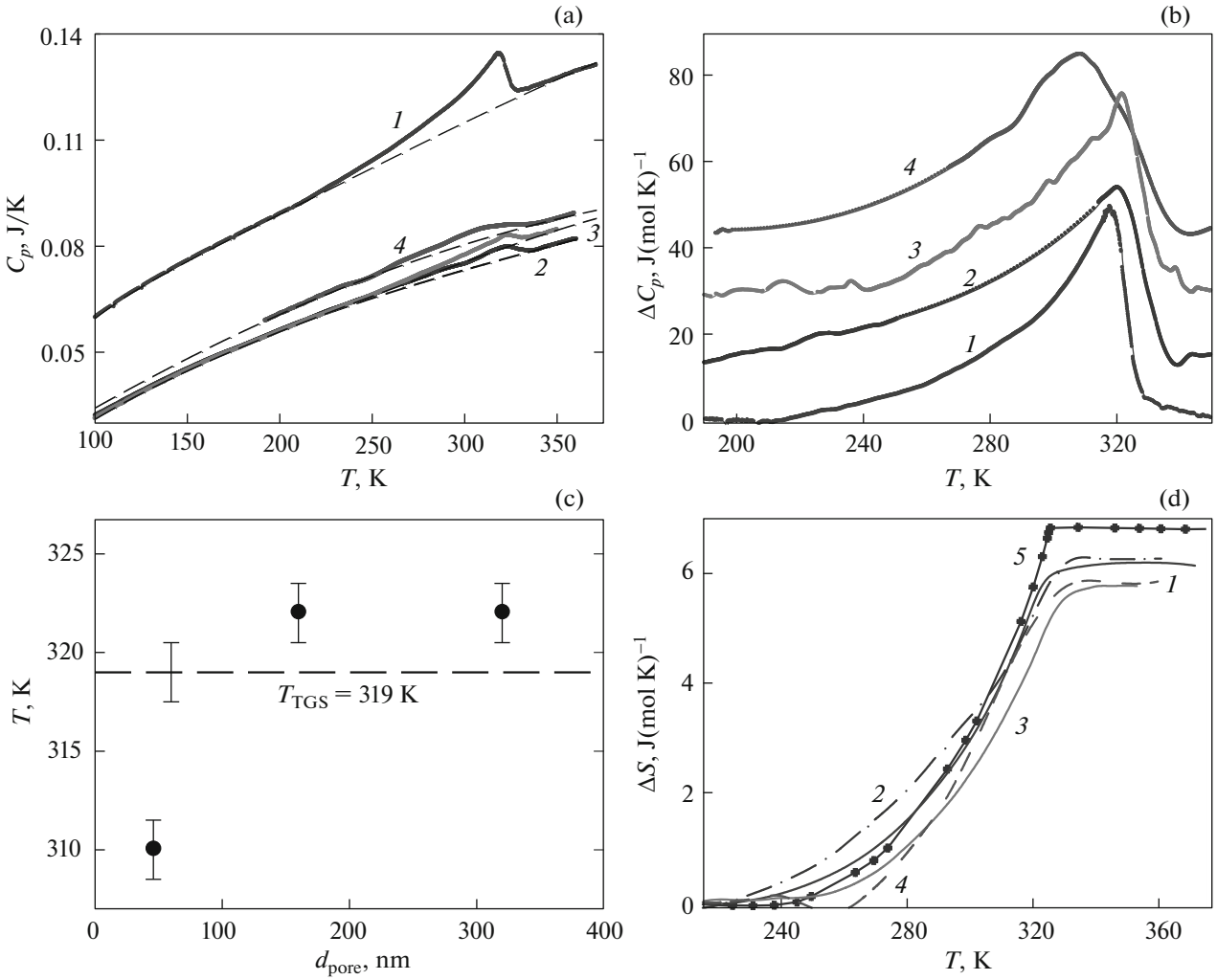

Fig. 2. Temperature dependences of specific heat of (*1*) ceramic TGS, (*2*) TGS + PG320, (*3*) TGS + PG160, and (*4*) TGS + PG46 composites, (b) anomalous heat capacity, and (d) phase transition entropy. Dashed lines in (a) show the regular component of specific heat. Curves *2*, *3*, and *4* are shifted upward by 15, 30, and 45 J (mol K)$^{-1}$, respectively. (c) Phase transition temperatures in the composites. (d) Entropy data on single-crystal TGS (*5*) borrowed from [19].

mal expansion coefficients, the error on determination of these coefficients was significant: 20% for PG and 8% for the composites. However, the discrepancy between the data obtained in sequential measurement series was no larger than ~5%.

3. RESULTS AND DISCUSSION

The results of experimental studies on the specific heat of the composites and ceramic TGS are illustrated in Fig. 2a. The $C_p(T)$ dependences of all the samples contain anomalies related to the phase transition in TGS, which spreads with a decrease in the pore size.

To extract the anomalous contribution $\Delta C_p(T)$ to the specific heat of the ferroelectric component and determine the integral characteristics of the phase transition, the specific heat of the TGS + PG composites far from T_C was considered to be a regular C_{LAT} contribution. The results of approximation of these data by a polynomial function are shown by the dashed line in Fig. 2a.

The experimental temperature dependences of the anomalous specific heat were recalculated into the TGS molar specific heat $\Delta C_p(T)$, which is presented in Fig. 2b. It can be seen that the temperature range of the presence of ΔC_p and its value slightly change with the PG pore size. Taking the ΔC_p maximum temperature to be T_C, we can see that the phase transition in the TGS + PG320 and TGS + PG160 composites occurs at a temperature higher by 3 K than T_C = 319.0 ± 1.5 K of quasi-ceramic TGS embedded in the matrix (Fig. 2c). On the other hand, as d_{pore} further decreases to 46 nm, T_C decreases by 12 K.

Integrating the functions $(\Delta C_p/T)(T)$, we determined the entropy variations ΔS caused by the phase transition in the TGS component for all the TGS + PG composites under study, as well as for quasi-ceramic TGS (Fig. 2d). It can be seen that the ΔS values were smaller than the entropy determined for the single crystal $\Delta S_{cryst} = 6.78$ J/mol K [19]. The maximum difference was found to be ~18% for the TGS + PG160 and TGS + PG46 composites, which is greater than the measurement error in the experiments on the composites (±7%) and single crystal (±5%). The coincidence of transition entropies of the polycrystalline sample and TGS + PG320 composite is most likely due to the similarity of grain size and d_{pore}. Thus, TGS undergoing the second-order phase transition close to the tricritical point is characterized by a slight entropy drop under the conditions of limited geometry, in contrast to the NH_4HSO_4–glass composites, in which a decrease in d_{pore} in the same range led to a decrease in the ΔS_2 value by a factor of 1.5 as a result of the pronounced first-order transition [18].

Figure 3 shows temperature dependences of the linear thermal expansion coefficient α for the three TGS + PG composites and TGS ceramics. It can be seen that the $\alpha(T)$ behavior of the composites corresponds to the temperature dependence of the expansion coefficient of ceramic TGS. The absolute α values of the composites beyond the transition region ~$(0.9–1.2) \times 10^{-5}$ K^{-1} are higher than $\alpha \approx (1–4) \times 10^{-6}$ K^{-1} PG and, as expected, appeared smaller than $\alpha \approx (1.7–3.2) \times 10^{-5}$ K^{-1} for TGS ceramics. The values of Δα anomalies caused by the phase transition in the TGS component decreased by almost an order of magnitude as compared with the quasi-ceramic sample.

The temperatures of the $\alpha(T)$ maxima considered to be T_C agree satisfactorily with the transition temperatures determined from the $(\Delta C_p)(T)$ dependences. Thus, on the one hand, the phase transition in the TGS + PG320 and TGS + PG160 composites occurs at a temperature slightly higher than T_C for quasi-ceramic TGS and, on the other hand, the T_C value significantly decreases with a further decrease in d_{pore} (Fig. 2c). These data agree qualitatively with the results obtained when studying the permittivity of some TGS + PG composites [17]. The similar behavior of the phase transition temperatures was observed in the NH_4HSO_4–glass composites [18].

We may suggest the existence of two mechanisms of the pore size effect on the phase transition temperature of TGS embedded in the glass matrix. One of them is related to the large difference between the TGS and PG thermal expansion coefficients ($\alpha_{TGS} \gg \alpha_{PG}$), which leads to the occurrence of tensile stresses in the ferroelectric component. This mechanism probably plays a key role in the samples with $d_{cryst} >$ 100 nm. In TGS, the transition temperature increases

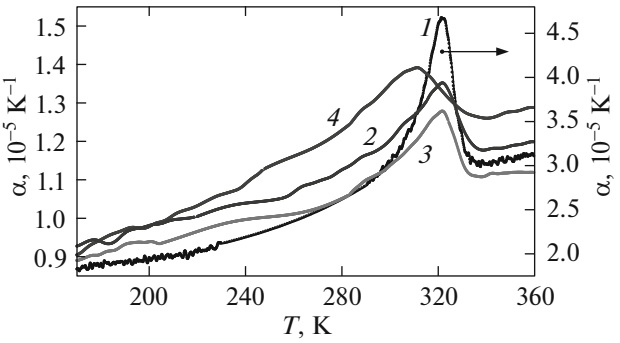

Fig. 3. Temperature dependences of the coefficient of linear thermal expansion of ceramic TGS (*1*) and TGS + PG320 (*2*), TGS + PG160 (*3*), and TGS + PG46 (*4*) composites.

with the pressure ($dT_C/dp = 2.6$ K/kbar) [23, 24] and the tensile stresses should lead to a decrease in the transition temperature in the composites compared to T_C of quasi-ceramic TGS. However, the low pressure coefficient and small difference between the temperatures of glass filling (~340 K) and phase transition (~320 K) in ceramic TGS should not lead to a significant change in the temperature of the ferroelectric transition in the composites due to this effect. At the same time, the observed decrease in the unit cell volume of embedded TGS as compared with the free bulk crystal (Table 1) is indicative of the presence of compressive stresses, which can lead to a slight increase in the transition temperature at $dT_C/dp > 0$. It is difficult to prefer one of the interaction variants, since the T_C growth by only ~3 K in the TGS + PG320 and TGS + PG160 composites is comparable with the total error of determination of the temperature of spread specific heat anomalies and thermal expansion in both the ceramic and composite samples.

The other mechanism of the phase transition temperature variation in ferroelectric nanoparticles is related to the changes in the balance of long- and short-range interactions [25–27]. We can state with confidence that this mechanism plays a decisive role in the composites with small particle sizes ($d_{cryst} <$ 100 nm), leading to a decrease in T_C with decreasing d_{cryst}.

With the ΔC_p and Δα data at T_C, we can calculate the second-order phase transition temperature shift under hydrostatic pressure using the Ehrenfest equation $dT/dp = T_C(\Delta\beta/\Delta C_p)$, where $\beta = 3\alpha$ for isotropic materials (ceramics and composites). The pressure coefficients dT/dp calculated for the ceramic sample and TGS + PG320 composite were found to be 6 and 0.9 K/kbar, respectively. Taking into account the small shift of the transition temperature under pressure, the ratio between the calculated dT/dp values and an experimental value of 2.6 K/kbar for the TGS single crystal as can be considered [23] satisfactory. In addition, the

expantion coefficient of the composites is determined at the ratio $\beta = (1/V_{TGS+PG})(\Delta V_{TGS+PG}/\Delta T)$ between the volume and its temperature change. If we attribute the variation ΔV_{TGS+PG} to the embedded TGS volume, then the value $dT/dp = 3$ K/kbar agrees satisfactorily with the experimental value.

4. CONCLUSIONS

The effect of limited geometry on specific heat and thermal expansion of the TGS–borosilicate glass composites was studied first. The nonmonotonic variation in the phase transition temperature $P2_1 \leftrightarrow P2_1/m$ accompanied by a slight increase in the TGS + PG320 and TGS + PG160 composites and a significant decrease in the TGS + PG46 composites was observed, which agrees qualitatively with the data reported in [17]. A slight change in the anomalous values of the specific heat and thermal expansion coefficient during the phase transition in TGS at the change in the glass matrix pore diameter was established. To a greater extent there is a decrease in the transition entropy with decreasing d_{pore}, but even in the TGS + PG46 composite the ΔS value remains typical of the order–disorder transformations. The calculations for the composites showed the minor effect of internal pressure on the pressure coefficient.

Thus, the thermal properties at the second-order transformation in TGS close to the tricritical point are weakly affected by the limited space than the properties of NH_4HSO_4 [18], which undergoes the strong first-order transformation $P1 \leftrightarrow P_c$.

ACKNOWLEDGMENTS

The authors thank S.D. Milovidova for help in synthesizing the nanocomposites.

This study was supported by the Russian Foundation for Basic Research, project no. 16-32-00092 mol-a.

REFERENCES

1. Y. Kumzerov and S. Vakhrushev, Encycl. Nanosci. Nanotechnol. **10**, 1 (2003).
2. M. I. Bichurin and V. M. Petrov, J. Low Temp. Phys. **36**, 544 (2010).
3. E. A. Mikhaleva, I. N. Flerov, A. V. Kartashev, M. V. Gorev, A. V. Cherepakhin, K. A. Sablina, N. V. Mikhashonok, N. V. Volkov, and A. V. Shabanov, J. Mater. Res. **28**, 3322 (2013).
4. E. Mikhaleva, E. Eremin, I. Flerov, A. Kartashev, K. Sablina, and N. Mikhashenok, J. Mater. Res. **30**, 278 (2015).
5. Z. Kutnjak, B. Vodopivec, R. Blinc, A. V. Fokin, Y. A. Kumzerov, and S. B. Vakhrushev, J. Chem. Phys. **123**, 084708 (2005).
6. S. B. Vakhrushev, I. V. Golosovskii, E. Yu. Koroleva, A. A. Naberezhnov, N. M. Okuneva, O. P. Smirnov, A. V. Fokin, M. Tovar, and M. Glazman, Phys. Solid State **50**, 1548 (2008).
7. Yu. A. Kumzerov, N. F. Kartenko, L. S. Parfen'ev, I. A. Smirnov, A. V. Fokin, D. Wlosewicz, H. Misiorek, and A. Jezowski, Phys. Solid State **53**, 1099 (2011).
8. V. Tarnavich, L. Korotkov, O. Karaeva, A. Naberezhnov, and E. Rysiakiewicz-Pasek, Opt. Appl. **40**, 305 (2010).
9. A. Ciżman, T. Marciniszyn, and R. Poprawski, J. Appl. Phys. **112**, 034104 (2012).
10. O. V. Rogazinskaya, S. D. Milovidova, A. S. Sidorkin, N. G. Popravko, M. A. Bosykh, and V. S. Enshina, Ferroelectrics **397**, 191 (2010).
11. N. G. Popravko, A. S. Sidorkin, S. D. Milovidova, and O. V. Rogazinskaya, Ferroelectrics **443**, 8 (2013).
12. S. D. Milovidova, A. S. Sidorkin, O. V. Rogazinskaya, and E. V. Vorotnikov, Ferroelectrics **497**, 69 (2016).
13. O. M. Golitsyna, S. N. Drozhdin, A. E. Gridnev, V. V. Chernyshev, and I. E. Zanin, Bull. Russ. Acad. Sci.: Phys. **74**, 1291 (2010).
14. A. Fokin, Yu. Kumzerov, E. Koroleva, A. Naberezhnov, O. Smirnov, M. Tovar, S. Vakhrushev, and M. Glazman, J. Electroceram. **22**, 270 (2009).
15. O. M. Golitsyna, S. N. Drozhdin, I. E. Zanin, and A. E. Gridnev, Phys. Solid State **54**, 2296 (2012).
16. S. V. Baryshnikov, E. V. Charnaya, E. V. Stukova, and A. Yu. Milinskii, Cheng Tien, Phys. Solid State **52**, 1444 (2010).
17. A. Cizman, T. Antropova, I. Anfimova, I. Drozdova, E. Rysiakiewicz-Pasek, E. B. Radojewska, and R. Poprawski, J. Nanopart. Res. **15**, 1807 (2013).
18. E. A. Mikhaleva, I. N. Flerov, A. V. Kartashev, M. V. Gorev, E. V. Bogdanov, V. S. Bondarev, L. N. Korotkov, and E. Rysiakiewicz-Pasek, Ferroelectrics **513**, 44 (2017).
19. B. A. Strukov, E. P. Ragula, S. V. Arkhangel'skaya, and I. V. Shnaidshtein, Phys. Solid State **40**, 94 (1998).
20. A. Gutina, T. Antropova, E. Rysiakiewicz-Pasek, K. Virnik, and Yu. Feldman, Microporous Mesoporous Mater. **58**, 237 (2003).
21. Bruker AXS TOPAS V4, *General Profile and Structure Analysis Software for Powder Diffraction Data—User's Manual* (Bruker AXS, Karlsruhe, Germany, 2008).
22. A. V. Kartashev, I. N. Flerov, N. V. Volkov, and K. A. Sablina, Phys. Solid State **50**, 2115 (2008).
23. G. G. Leonidova, I. N. Polandov, and I. P. Golentovskaya, Sov. Phys. Solid State **4**, 2443 (1962).
24. Y. Kobayashi, S. Sawada, H. Furuta, S. Endo, and K. Deguchi, J. Phys.: Condens. Matter **14**, 11139 (2002).
25. R. Kretschmar and K. Binder, Phys. Rev. B **20**, 1065 (1979).
26. D. R. Tilley and B. Zeks, Solid State Commun. **49**, 823 (1984).
27. K. Ishikawa, K. Yoshikawa, and N. Okada, Phys. Rev. B **37**, 5852 (1988).

Translated by E. Bondareva